AIMS Mathematics, 7(6): 10344–10363.
DOI: 10.3934/math.2022576
Received: 05 November 2021
Revised: 05 November 2021
Accepted: 20 February 2022
Published: 25 March 2022

http://www.aimspress.com/journal/Math

Research article

An effective approach based on Hybrid B-spline to solve Riesz space fractional partial differential equations

M. S. Hashmi[1], Rabia Shikrani[1], Farwa Nawaz[1], Ghulam Mustafa[2], Kottakkaran Sooppy Nisar[3,*] and Velusamy Vijayakumar[4]

[1] Department of Mathematics, The Government Sadiq College Women University, Bahawalpur, Pakistan
[2] Department of Mathematics, The Islamia University of Bahawalpur, Pakistan
[3] Department of Mathematics, College of Arts and Sciences, Wadi Aldawaser, Prince Sattam bin Abdulaziz University, Saudi Arabia
[4] Department of Mathematics, School of Advanced Sciences, Vellore Institute of Technology, Vellore-632014, Tamilnadu, India

* **Correspondence:** Email: n.sooppy@psau.edu.sa

Abstract: B-spline is extensively used for the solution of many physical models appearing in the fields of plasma physics, fluid mechanics, atmosphere-ocean dynamics and many other disciplines. In this article, Riesz space fractional PDEs (RSF-PDEs) in two forms are solved by using hybrid B-spline collocation method (HBCM). In the given methodology, RSF-PDEs are discretized into the system of algebraic linear equations by using hybrid B-spline basis function. The resultant system is solved by a numerical technique. The Von Neumann stability analysis method is used for analyzing the stability of proposed method. Numerical experiments are conducted to illustrate the accuracy of proposed method, by representing the results graphically and numerically for different values of fractional parameters.

Keywords: collocation method; fractional PDE; B-spline functions; numerical method; Von Neumann stability analysis
Mathematics Subject Classification: 35R11, 41A15

1. Introduction

In many areas of the modern life, mathematical modeling and numerical outcomes are integrated. Most of the mathematical methods, which can be used in engineering and natural sciences are based on ordinary differential equations (ODEs), partial differential equations (PDEs) and integral equations (IEs). Many fields of engineering and sciences including probability theory, fluid flow and

electromagnetic theory represent the advantages of fractional equations over the ordinary equations [1–3].

Fractional differential equations have rich physical background in different fields of sciences. Fractional derivative provides an adequate approach to describe the physical models, which preserve the memory and hereditary properties of physical substances. This versatility of fractional derivative makes it more applicable in the field of physics [4], biology [5], hydrology [6] and chemistry [7]. More expressly, they are used in dynamical systems with quasi-chaotic behaviour, chaotic dynamical behavior, porous media or dynamics of complex material. Now-a-days, the interest of some of the scholars have been demonstrated in the form of research on the study of mathematical theory of fractional differential equations [8–10].

Among various definitions of fractional derivative, the Riesz fractional derivative involves a sum of the Riemann-Liouville right- and left- sided derivatives. This induction facilitates to describe the impact of fluid flow on both sides of the domain. The Riesz space fractional PDE was derived by Saichev and Zaslavsky [11] from the kinetics of chaotic dynamics. The kinetic equation with the fractional derivatives are considered for the non-negative values of K_α, K_β in order to observe the flow from left to right. The discretized version of the Riesz fractional derivative in space can facilitate the solution of inconsistency problem. One of the general form of the Riesz space fractional diffusion equation (RSF-DE) [12] for $1 < \alpha \leqslant 2$ is

$$\frac{\partial G(x,t)}{\partial t} = K_\alpha \frac{\partial^\alpha G(x,t)}{\partial |x|^\alpha} + f(x,t), \quad K_\alpha \geqslant 0,\ 0 < t \leqslant T, a < x < b, \tag{1.1}$$

with boundary conditions $G(a,t) = G(b,t) = 0$, initial condition $G(x,0) = \psi(x)$ and here K_α is diffusion coefficient.

Let us consider the Riesz space fractional advection dispersion equation (RSF-ADE) [12] for $1 < \alpha \leqslant 2$ and $0 < \beta < 1$ as

$$\frac{\partial G(x,t)}{\partial t} = K_\alpha \frac{\partial^\alpha G(x,t)}{\partial |x|^\alpha} + K_\beta \frac{\partial^\beta G(x,t)}{\partial |x|^\beta} + f(x,t), \quad K_\alpha, K_\beta \geqslant 0,\ 0 < t \leqslant T, a < x < b, \tag{1.2}$$

with boundary conditions $G(a,t) = G(b,t) = 0$ and initial condition $G(x,0) = \psi(x)$, where α, β are fractional parameters, K_α, K_β represent the dispersion coefficient and average fluid velocity, $G(x,t)$ is an unknown function of space and time, $\psi(x)$ is a continuous functions and $f(x,t)$ is a source term.

The Riesz fractional operator on a finite interval $0 \leqslant x \leqslant L$ for $n-1 < \alpha \leqslant n$ (n is positive integer and L is a real number) is described as

$$\begin{aligned}
\frac{\partial^\alpha G(x,t)}{\partial |x|^\alpha} &= -C_\alpha \left({}_0D_x^\alpha + {}_xD_L^\alpha\right) G(x,t) = -\frac{C_\alpha}{h^\alpha} \left(\sum_{p=0}^{m+1} w_p^\alpha G_{m-p+1}^{n+1} + \sum_{p=0}^{N-m+1} w_p^\alpha G_{m+p-1}^{n+1} \right) + O(h), \\
\frac{\partial^\beta G(x,t)}{\partial |x|^\beta} &= -C_\beta \left({}_0D_x^\beta + {}_xD_L^\beta\right) G(x,t) = -\frac{C_\beta}{h^\beta} \left(\sum_{p=0}^{m} w_p^\beta G_{m-p}^{n+1} + \sum_{p=0}^{N-m} w_p^\beta G_{m+p}^{n+1} \right) + O(h),
\end{aligned}$$

where

$$C_\nu = \frac{1}{2\cos(\frac{\pi\nu}{2})}, \nu \neq 1 \text{ for } \nu \in \{\alpha, \beta\}.$$

Here $x_i = a + ih, i = 0, 1, 2, \ldots, N, h = \frac{b-a}{N}$, $G^{n+1}_{m+p-1} = G(x_{m+p-1}, t_{n+1})$, $w^{\nu}_0 = 1, w^{\nu}_p = \frac{(-1)^{\nu}\nu(\nu-1)\cdots(\nu-p+1)}{p!}$, $p = 1, 2, \ldots, \nu \in \{\alpha, \beta\}$. Moreover ${}_0D^{\nu}_x$ and ${}_xD^{\nu}_L$ for $\nu \in \{\alpha, \beta\}$ are Riemann-Liouville left and right sided derivatives [12].

Several numerical techniques have been used to solve RSF-PDEs, Shen et al. [13] have worked over the fundamental solution of RSF-ADE using Laplace and Fourier transforms methods. Zhang et al. [14] have proposed a backward difference scheme and a finite element method to solve a symmetric Space fractional PDE with the Riesz fractional operator and Riemann-Liouville discretization. Ding et al. [15] have introduced a new numerical method, in which they proved its effectiveness for Reisz problem. Liao et al. [16] has used second order BDF approximation for the solution of RSF-DE, a series of fast parallel preconditioning methods based on implicit technique for the solution of said equation has been utilized by Gu et al. [17, 18]. Jian et al. [19–21] used as fast iterative methods for the solution of fractional reaction diffusion and convection reaction diffusion equation.

From the existing results, it has been seen that spline functions have been used to solve DEs. Zahra and Elkholy [22] presented a numerical solution of FDEs by the use of cubic splines. Non classical diffusion problems by Abbas et al. [23], advection-diffusion problems by Nazir et al. [24] and fractional sub-diffusion equation by Zhu et al. [25] are solved by using B-spline collocation method. Yaseen et al. [26] presented a finite difference scheme based on cubic trigonometric B-splines for a time fractional diffusion-wave equation. Hashmi et al. [27] has solved Hunter-Saxton equation by using cubic trigonometric B-spline collocation method. Most recently, B-spline based collocation method [28, 29] and differential quadrature method have been applied by Hashmi et al. [30, 31] for the solution of fractional PDEs.

From the existing results, it is evident that no attempt has been made to solve RSF-PDEs using HBCM. In present research, formulation of Riesz space fractional derivatives using the Riemann Liouville right and left sided derivatives, indebted with HBCM has been used. Von Neumann stability analysis approach is used to achieve the convergence, which shows that our proposed method is unconditionally stable. Numerical examples with their tabular and graphical representations are included to illustrate the efficiency of proposed method.

The layout of this paper is as follows: HBCM is given in Section 2. In Section 3, temporal discretization, proposed methodology and convergence analysis of RSF-DE is presented. In Section 4 temporal discretization of RSF-ADE along with proposed method is presented and demonstrated with examples. The conclusion of the proposed technique for both models is discussed in last section.

2. Hybrid B-spline collocation method

Let τ be the time step such that $t_n = n\tau$, $n = 0, 1, 2, \ldots, M$, i.e. $0 \leqslant t_n \leqslant T$, and h is the step size with $x_m = a + mh, a \leqslant x_m \leqslant b, m = 0, 1, 2, \ldots, N$. Let G^n_m be the numerical estimate of $G(x, t)$ at the mesh point (x_m, t_n). Now HBCM is used to solve the FPDEs. The approximate solution of $G(x, t)$ is considered as

$$G(x, t) = \sum_{j=-1}^{N+1} C_j(t) H_{3,j}(x) \tag{2.1}$$

where $C_j(t)$ are unknown parameters and $H_{3,j}(x)$ is hybrid cubic B-spline basis function of order three and described as

$$H_{3,j}(x) = \gamma B_{3,j}(x) + (1 - \gamma) T_{3,j}(x), \tag{2.2}$$

where $\gamma = 1$ and $\gamma = 0$, represent the cubic B-spline basis $B_{3,j}(x)$ and trigonometric B-spline basis $T_{3,j}(x)$ function respectively. For Hybrid bases, Table 1 represents the functional values of the hybrid B-spline: Here

Table 1. Functional values of $H_{3,j}(x)$ and its derivatives at its nodes.

x	x_{j-2}	x_{j-1}	x_j	x_{j+1}	x_{j+2}
$H_{3,j}$	0	R_1	R_2	R_1	0
$H'_{3,j}$	0	R_3	0	$-R_3$	0
$H''_{3,j}$	0	R_4	R_5	R_4	0

$$R_1 = \frac{\gamma}{6} + (1-\gamma)r_1\,, \qquad R_2 = \frac{2\gamma}{3} + (1-\gamma)r_2\,,$$
$$R_3 = \frac{\gamma}{2h} + (1-\gamma)r_3\,, \qquad R_4 = \frac{\gamma}{h^2} + (1-\gamma)r_4\,,$$
$$R_5 = -\frac{2\gamma}{h^2} + (1-\gamma)r_5$$

and

$$r_1 = \frac{\sin^2(\frac{h}{2})}{\sin(h)\sin(\frac{3h}{2})}\,, \quad r_2 = \frac{2}{1+2\cos(h)}\,, \quad r_3 = -\frac{3}{4\sin(\frac{3h}{2})}\,,$$
$$r_4 = \frac{3}{4\sin(\frac{3h}{2})}\,, \quad r_5 = \frac{3(1+3\cos(h))}{16\sin^2(\frac{h}{2})(2\cos(\frac{h}{2})+\cos(\frac{3h}{2}))}\,,$$
$$r_6 = -\frac{3\cos^2(\frac{h}{2})}{\sin^2(\frac{h}{2})(2+4\cos(h))}\,.$$

The B-spline representation of $G(x,t)$ with its derivatives at (x_m, t_{n+1}) have the form

$$\begin{cases} G_m^{n+1} = R_1 C_{m-1}^{n+1} + R_2 C_m^{n+1} + R_1 C_{m+1}^{n+1}\,, \\ (G_x)_m^{n+1} = R_3 C_{m-1}^{n+1} - R_3 C_{m+1}^{n+1}\,, \\ (G_{xx})_m^{n+1} = R_4 C_{m-1}^{n+1} + R_5 C_m^{n+1} + R_4 C_{m+1}^{n+1}\,. \end{cases} \tag{2.3}$$

3. Riesz space fractional diffusion equation (RSF-DE)

FPDEs are undergoing rapid development due to their wide application in engineering, economics and physics. In the present research, RSF-DE is solved by using HBCM. The proposed methodology is as follows:

3.1. Proposed methodology

The time derivative and the Riesz fractional derivatives are discretized by implicit Euler scheme and the shifted Grunwald formulae respectively, in order to apply HCBM on (1.1) as follows:

$$\frac{G_m^{n+1} - G_m^n}{\tau} = -\frac{K_\alpha}{2\cos(\frac{\pi\alpha}{2})h^\alpha}\left(\sum_{p=0}^{m+1} w_p^\alpha G_{m-p+1}^{n+1} + \sum_{p=0}^{N-m+1} w_p^\alpha G_{m+p-1}^{n+1}\right) + f_m^n, \tag{3.1}$$

simplifying (3.1) with the help of (2.3), the resultant equation becomes

$$\begin{aligned}&(R_1C_{m-1}^{n+1}+R_2C_m^{n+1}+R_1C_{m+1}^{n+1})-(R_1C_{m-1}^{n}+R_2C_m^{n}+R_1C_{m+1}^{n})\\&+\eta\Bigg(\sum_{p=0}^{m+1}w_p^{\alpha}(R_1C_{m-p}^{n+1}+R_2C_{m-p+1}^{n+1}+R_1C_{m-p+2}^{n+1})\\&+\sum_{p=0}^{N-m+1}w_p^{\alpha}(R_1C_{m+p-2}^{n+1}+R_2C_{m+p-1}^{n+1}+R_1C_{m+p}^{n+1})\Bigg)+\tau f_m^n=0\end{aligned}\tag{3.2}$$

where $\eta=\frac{K_\alpha\tau}{2\cos(\frac{\pi\alpha}{2})h^\alpha}$ and $w_0^\alpha=0$. For $(m=0,\ldots,N)$, the above equation provides a rectangular system of unknowns. So the BCs are used to obtained two more additional constraints for finding a unique solution of the system described, which are given below

$$G(x_0,t_{n+1}) = R_1C_{-1}^{n+1}+R_2C_0^{n+1}+R_1C_1^{n+1}=0,\tag{3.3}$$

$$G(x_N,t_{n+1}) = R_1C_{N-1}^{n+1}+R_2C_N^{n+1}+R_1C_{N+1}^{n+1}=0.\tag{3.4}$$

Now the obtained system can be solved by a variant of Thomas algorithm.

3.2. Initial state

First, we will find an initial vector to start the iterative process i.e. $C^0=[C_{-1}^0,C_0^0,\ldots,C_{N+1}^0]^T$. This can be determined by utilizing the IC on the approximate solution

$$G(x,0)=\sum_{m=-1}^{N+1}C_m(0)H_{3,m}(x)\tag{3.5}$$

where $C_m(0)'s$ are unknown parameters. Here $G(x,0)$ is required, which satisfies the following conditions:

$$\begin{cases}G(x_m,0)=\psi(x_m)\\G_x(x_0,0)=\psi'(x_0)\\G_x(x_N,0)=\psi'(x_N)\end{cases}\qquad m=0,\ldots,N.\tag{3.6}$$

This can be written as $(N+3)\times(N+3)$ matrix system:

$$AC^0=B\tag{3.7}$$

where $C^0=[C_{-1}^0,C_0^0,\ldots,C_{N+1}^0]^t$,

$$A=\begin{pmatrix}R_3&0&-R_3&\ldots&\ldots&\ldots&\ldots&0\\R_1&R_2&R_1&\ddots&&&&\vdots\\0&R_1&R_2&R_1&\ddots&&&\\\vdots&&&&\ddots&&&\vdots\\\vdots&&&&&R_1&R_2&R_1\\0&\ldots&\ldots&\ldots&\ldots&R_3&0&-R_3\end{pmatrix}$$

and $B=[\psi'(x_0),\psi(x_0),\ldots,\psi(x_N),\psi'(x_N)]^t$. This will provide us a starting solution to the iterative process given in (3.2)–(3.4).

3.3. Stability analysis

The stability analysis is performed using Von Neumann stability analysis in terms of evaluation of amplitude of the error. For this, we considered the homogenous problem, it is as follows:

$$C_m^n = \xi_n e^{im\phi h}, \tag{3.8}$$

where m and ϕ are real numbers. By substituting (3.8) in (3.1) and simplifying, we have

$$\begin{aligned}&\xi_{n+1}(2R_1\cos(\phi h)+R_2)-\xi_n(2R_1\cos(\phi h)+R_2)\\&+\eta\left(\sum_{p=0}^{m+1} w_p^{\alpha} e^{(-p+1)i\phi h}\xi_{n+1}(2R_1\cos(\phi h)+R_2)\right.\\&\left.+\sum_{p=0}^{N-m+1} w_p^{\alpha} e^{(p-1)i\phi h}\xi_{n+1}(2R_1\cos(\phi h)+R_2)\right)=0.\end{aligned} \tag{3.9}$$

The Eq (3.9) can be re-written as

$$\xi_{n+1} \;=\; \frac{1}{(1+C_1+C_2)}\xi_n, \tag{3.10}$$

where

$$C_1=\eta\sum_{p=0}^{m+1} w_p^{\alpha} e^{(-p+1)i\phi h} \;\text{ and }\; C_2=\eta\sum_{p=0}^{N-m+1} w_p^{\alpha} e^{(p-1)i\phi h}. \tag{3.11}$$

Now the relation has the form

$$\xi_{n+1}\leqslant\frac{1}{\nu}\xi_n,\;\; \text{where}\;\; \nu=1+C_1+C_2 \qquad \text{and} \qquad \nu>1. \tag{3.12}$$

It concludes that the system is unconditionally stable.

3.4. Convergence of the scheme

The convergence estimates for the proposed scheme is presented here for the homogenous case:

Theorem 3.1. *Let $\{G(x,t^n)\}_{n=0}^{M}$ be the exact solution of the problem and let $\{G^n\}$ be the approximate solution of proposed problem then*

$$\|e^{n+1}\|\leqslant\frac{1}{D}\|e^n\|$$

where $e^{n+1}=\{|G(x_m,t^{n+1})-G_m^{n+1}|;\;\; m=0,1,\ldots,N\}$ and $D=\left(1+\eta\sum\limits_{p=0}^{m+1} w_p^{\alpha}+\eta\sum\limits_{p=0}^{N-m+1} w_p^{\alpha}\right)$.

Proof. For $h>0$, we know that $R_1=\frac{\gamma}{6}+(1-\gamma)r_1, R_2=\frac{2\gamma}{3}+(1-\gamma)r_2$, then:

- For $\gamma=1$ implies $R_1=\frac{1}{6}, R_2=\frac{2}{3}$ implies $R_2>R_1$
- For $\gamma=0$ implies $R_1=\frac{\sin^2(\frac{h}{2})}{\sin(h)\sin(\frac{3h}{2})}, R_2=\frac{2}{1+2\cos(h)}$ implies $R_2>R_1$ for all $h>0$ in the domain of the problem. This results that the coefficient matrix A given in (3.7) is strictly diagonally dominant and will produce a unique solution.

For the proposed problem, let the exact solution satisfies the numerical scheme (3.1), then we have

$$\frac{G(x_m,t_{n+1})-G(x_m,t_n)}{\tau}=-\frac{K_\alpha}{2\cos(\frac{\pi\alpha}{2})h^\alpha}\left(\sum_{p=0}^{m+1}w_p^\alpha G(x_{m-p+1},t^{n+1})+\sum_{p=0}^{N-m+1}w_p^\alpha G(x_{m+p-1},t^{n+1})\right),$$

or

$$G(x_m,t_{n+1})-G(x_m,t_n)=-\eta\left(\sum_{p=0}^{m+1}w_p^\alpha G(x_{m-p+1},t^{n+1})+\sum_{p=0}^{N-m+1}w_p^\alpha G(x_{m+p-1},t^{n+1})\right),$$

and then the approximate solution will have the form

$$G_m^{n+1}-G_m^n=-\eta\left(\sum_{p=0}^{m+1}w_p^\alpha G_{m-p+1}^{n+1}+\sum_{p=0}^{N-m+1}w_p^\alpha G_{m+p-1}^{n+1}\right),$$

subtracting above two equations gives

$$e^{n+1}=e^n-\eta\left(\sum_{p=0}^{m+1}w_p^\alpha e^{n+1}+\sum_{p=0}^{N-m+1}w_p^\alpha e^{n+1}\right),$$

where $e^{n+1}=\max\{|G(x_m,t^{n+1})-G_m^{n+1}|;\ \ m=0,1,\ldots,N\}$. Taking the inner product with e^{n+1} on both sides and using the fact that $\langle y,y\rangle=\|y\|^2$, we have

$$\begin{aligned}
\langle e^{n+1},e^{n+1}\rangle &= \langle e^n,e^{n+1}\rangle-\eta\left(\sum_{p=0}^{m+1}w_p^\alpha\langle e^{n+1},e^{n+1}\rangle+\sum_{p=0}^{N-m+1}w_p^\alpha\langle e^{n+1},e^{n+1}\rangle\right),\\
\|e^{n+1}\|^2 &= \langle e^n,e^{n+1}\rangle-\eta\left(\sum_{p=0}^{m+1}w_p^\alpha\|e^{n+1}\|^2+\sum_{p=0}^{N-m+1}w_p^\alpha\|e^{n+1}\|^2\right),\\
\|e^{n+1}\|^2 &\leqslant \|e^n\|\|e^{n+1}\|-\eta\left(\sum_{p=0}^{m+1}w_p^\alpha\|e^{n+1}\|^2+\sum_{p=0}^{N-m+1}w_p^\alpha\|e^{n+1}\|^2\right).
\end{aligned}$$

Dividing it by $\|e^{n+1}\|$ gives

$$\|e^{n+1}\| \leqslant \|e^n\|-\eta\left(\sum_{p=0}^{m+1}w_p^\alpha\|e^{n+1}\|+\sum_{p=0}^{N-m+1}w_p^\alpha\|e^{n+1}\|\right),$$

which means

$$\begin{aligned}
\|e^{n+1}\|\left(1+\eta\sum_{p=0}^{m+1}w_p^\alpha+\eta\sum_{p=0}^{N-m+1}w_p^\alpha\right) &\leqslant \|e^n\|,\\
\|e^{n+1}\| &\leqslant \frac{1}{D}\|e^n\|.
\end{aligned}$$

It is clear that $D\geqslant 1$, hence the proposed scheme is convergent. □

3.5. Example 1

In this example, HBCM is applied on RSF-DE to showcase the efficiency of proposed method. Consider an example of the form [12]

$$\frac{\partial G(x,t)}{\partial t} = -K_\alpha \frac{\partial^\alpha G(x,t)}{\partial |x|^\alpha} \tag{3.13}$$

with BCs $G(0,t) = 0, G(\pi,t) = 0$ and the IC $G(x,0) = x^2(\pi - x)$. The exact solution is $G(x,t) = \sum_{n=1}^{\infty} b_n sin(nx) e^{(-(n^2)^{\frac{\alpha}{2}} K_\alpha t)}$ where $b_n = \frac{8}{n^3}(-1)^{n+1} - \frac{4}{n^3}$.

Table 2 shows the absolute errors at different values of γ, which indicates that the results are acceptable for all choices of γ. Table 3 at $N = 2^4$ and Table 4 at $N = 2^6$ present the numerical display of absolute errors of the RSF-DE for different values of α. Similarly Table 5 describes the numerical display of errors for $N = 2^8$ at various values of α. From these taables, we concludes that proposed scheme has more convergent solutions for increasing values of N. Table 6 is providing the comparison between the spline collocation method and the solution obtained by [12]. In Figure 1(a–d), the geometrical display of absolute errors at different value of α has been illustrated, which indicates that the higher values of α provides the improved solution.

Table 2. The absolute errors for $N = 2^4$ of example 1 at $\alpha = 1.2$.

x	$\gamma = 0$	$\gamma = 0.5$	$\gamma = 1.0$
$\frac{\pi}{16}$	8.849960×10^{-5}	9.451300×10^{-5}	9.350890×10^{-5}
$\frac{3\pi}{16}$	4.415480×10^{-5}	4.465910×10^{-5}	4.457410×10^{-5}
$\frac{5\pi}{16}$	1.576210×10^{-5}	1.512030×10^{-5}	1.522870×10^{-5}
$\frac{7\pi}{16}$	8.183400×10^{-5}	8.087850×10^{-5}	8.104000×10^{-5}
$\frac{9\pi}{16}$	1.438941×10^{-4}	1.422872×10^{-4}	1.425587×10^{-4}
$\frac{11\pi}{16}$	1.915568×10^{-4}	1.883350×10^{-4}	1.888795×10^{-4}
$\frac{13\pi}{16}$	2.086891×10^{-4}	1.996169×10^{-4}	2.011500×10^{-4}
$\frac{15\pi}{16}$	1.673564×10^{-4}	5.385036×10^{-4}	4.192187×10^{-4}

Table 3. Numerical display of absolute errors of the RSF-DE for $N = 2^4$ of example 1 at different values of α.

	$\alpha = 1.6$			$\alpha = 1.8$		
x	Exact	Numerical	Error	Exact	Numerical	Error
0	0.000000	0.042532	4.253219×10^{-2}	0.000000	0.042407	4.240668×10^{-2}
$\frac{\pi}{4}$	1.453388	1.453358	2.938660×10^{-5}	1.453394	1.453355	3.899070×10^{-5}
$\frac{\pi}{2}$	3.875748	3.875850	1.013582×10^{-4}	3.875750	3.875849	9.873710×10^{-5}
$\frac{3\pi}{4}$	4.360192	4.360400	2.085417×10^{-4}	4.360185	4.360408	2.229866×10^{-4}
π	0.000000	−0.084675	8.467466×10^{-2}	0.000000	−0.084412	8.441232×10^{-2}

Table 4. Numerical display of errors of the RSF-DE for $N = 2^6$ of example 1 at different values of α.

	$\alpha = 1.6$			$\alpha = 1.8$		
x	Exact	Numerical	Error	Exact	Numerical	Error
0	0.000000	0.000256	2.557016×10^{-4}	0.000000	0.000212	2.124213×10^{-4}
$\frac{\pi}{4}$	1.453388	1.453359	2.895680×10^{-5}	1.453394	1.453355	3.930360×10^{-5}
$\frac{\pi}{2}$	3.875748	3.875849	1.005043×10^{-4}	3.875750	3.875849	9.870570×10^{-5}
$\frac{3\pi}{4}$	4.360192	4.360397	2.054763×10^{-4}	4.360185	4.360407	2.226424×10^{-4}
π	0.000000	−0.000666	6.664946×10^{-4}	0.000000	−0.000559	5.588218×10^{-4}

Table 5. Numerical display of errors of the RSF-DE for $N = 2^8$ of example 1 at different values of α.

	$\alpha = 1.6$			$\alpha = 1.8$		
x	Exact	Numerical	Error	Exact	Numerical	Error
0	0.000000	−0.000044	4.413990×10^{-5}	0.000000	−0.000052	5.159910×10^{-5}
$\frac{\pi}{4}$	1.453388	1.453359	2.888410×10^{-5}	1.453394	1.453355	3.955920×10^{-5}
$\frac{\pi}{2}$	3.875748	3.875849	1.002986×10^{-4}	3.875750	3.875849	9.875220×10^{-5}
$\frac{3\pi}{4}$	4.360192	4.360397	2.047472×10^{-4}	4.360185	4.360407	2.227451×10^{-4}
π	0.000000	−0.000425	4.245819×10^{-4}	0.000000	−0.000471	4.711657×10^{-4}

Table 6. Comparison of the maximum error example 1 of proposed scheme with the solution provided by [12].

$h = \pi/N$	MTM [12]	Proposed scheme
$\frac{\pi}{10}$	2.217(−2)	9.3934(−2)
$\frac{\pi}{20}$	5.759(−3)	2.1073(−2)
$\frac{\pi}{40}$	1.481(−3)	8.3915(−3)
$\frac{\pi}{80}$	3.727(−4)	1.7174(−3)

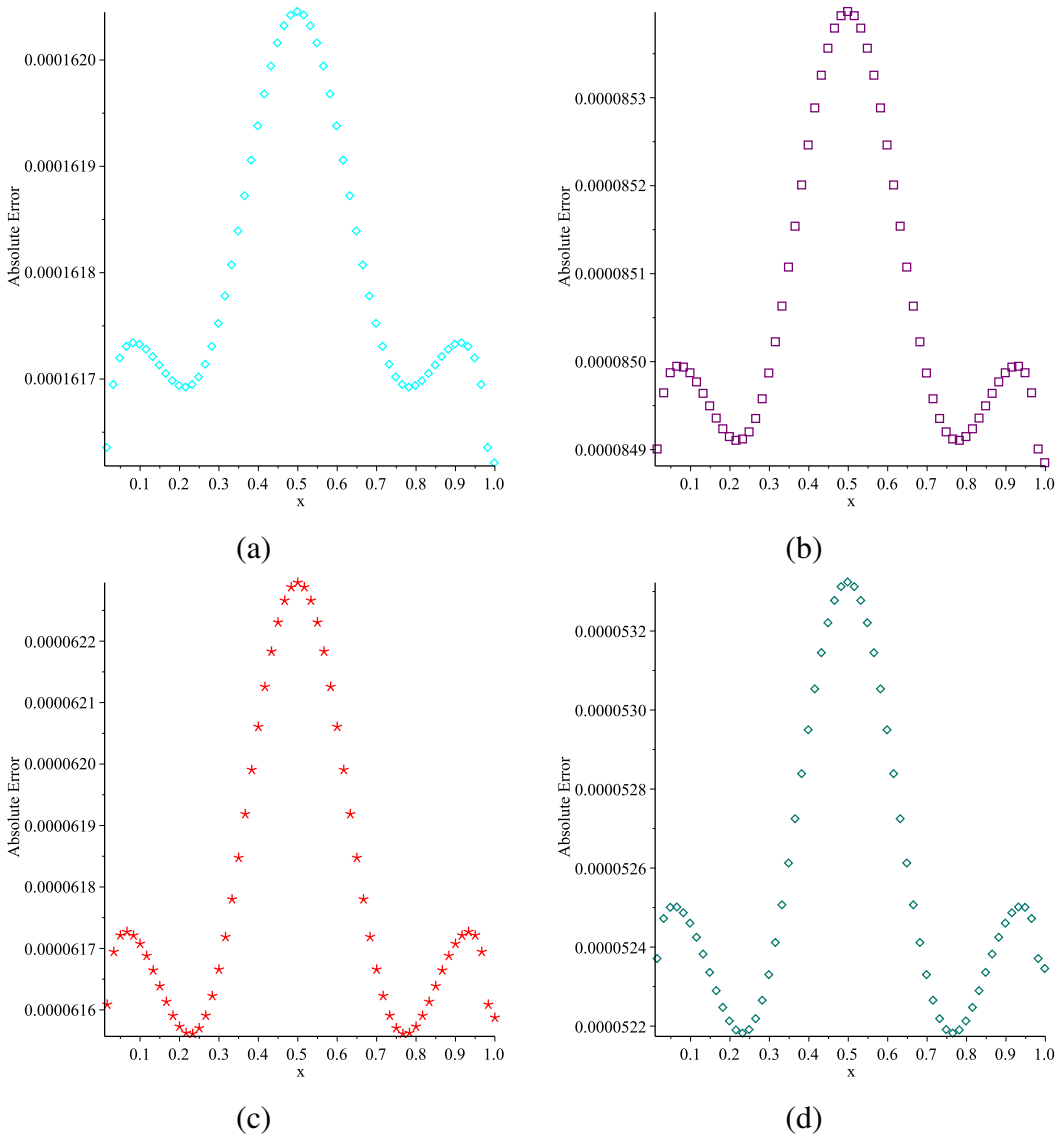

Figure 1. Represent geometrical display of absolute errors of example 1 for α = 1.2, 1.4, 1.6, 1.8 respectively.

4. Riesz space fractional advection-dispersion equation (RSF-ADE)

RSF-ADE is used in groundwater hydrology to model the transport of passive tracers carried by fluid flow in a porous medium. The space RSF-ADE have been used to describe important phenomena such as colloid, comb structures, bio-logical systems, glassy, disordered and porous media. In current section, the proposed methodology, stability analysis and numerical application of HBCM on RSF-ADE is performed.

4.1. Proposed methodology

Time derivative and RSF are discretized by implicit Euler scheme and shifted Grunwald formulae respectively in order to apply HBCM on (1.2) as follows:

$$\begin{aligned}\frac{G_m^{n+1}-G_m^n}{\tau} &= -\frac{K_\alpha}{2\cos(\frac{\pi\alpha}{2})h^\alpha}\left(\sum_{p=0}^{m+1} w_p^\alpha G_{m-p+1}^{n+1} + \sum_{p=0}^{N-m+1} w_p^\alpha G_{m+p-1}^{n+1}\right)\\ &\quad -\frac{K_\beta}{2\cos(\frac{\pi\beta}{2})h^\beta}\left(\sum_{p=0}^{m} w_p^\beta G_{m-p}^{n+1} + \sum_{p=0}^{N-m} w_p^\beta G_{m+p}^{n+1}\right) + f_m^n, \end{aligned} \tag{4.1}$$

re-arranging and simplifying we have

$$\begin{aligned}&G_m^{n+1} - G_m^n + \frac{K_\alpha\tau}{2\cos(\frac{\pi\alpha}{2})h^\alpha}\left(\sum_{p=0}^{m+1} w_p^\alpha G_{m-p+1}^{n+1} + \sum_{p=0}^{N-m+1} w_p^\alpha G_{m+p-1}^{n+1}\right)\\ &+\frac{K_\beta\tau}{2\cos(\frac{\pi\beta}{2})h^\beta}\left(\sum_{p=0}^{m} w_p^\beta G_{m-p}^{n+1} + \sum_{p=0}^{N-m} w_p^\beta G_{m+p}^{n+1}\right) - \tau f_m^n = 0. \end{aligned} \tag{4.2}$$

By substituting (2.3) in the above equation, we get

$$\begin{aligned}&(R_1C_{m-1}^{n+1} + R_2C_m^{n+1} + R_1C_{m+1}^{n+1}) - (R_1C_{m-1}^n + R_2C_m^n + R_1C_{m+1}^n)\\ &+\eta_1\left(\sum_{p=0}^{m+1} w_p^\alpha (R_1C_{m-p}^{n+1} + R_2C_{m-p+1}^{n+1} + R_1C_{m-p+2}^{n+1})\right.\\ &\left.+\sum_{p=0}^{N-m+1} w_p^\alpha (R_1C_{m+p-2}^{n+1} + R_2C_{m+p-1}^{n+1} + R_1C_{m+p}^{n+1})\right)\\ &+\eta_2\left(\sum_{p=0}^{m} w_p^\beta (R_1C_{m-p-1}^{n+1} + R_2C_{m-p}^{n+1} + R_1C_{m-p+1}^{n+1})\right.\\ &\left.+\sum_{p=0}^{N-m} w_p^\beta (R_1C_{m+p-1}^{n+1} + R_2C_{m+p}^{n+1} + R_1C_{m+p+1}^{n+1})\right) - \tau f_m^n = 0 \end{aligned} \tag{4.3}$$

where

$$\eta_1 = \frac{K_\alpha\tau}{2\cos(\frac{\pi\alpha}{2})h^\alpha} \quad \text{and} \quad \eta_2 = \frac{K_\beta\tau}{2\cos(\frac{\pi\beta}{2})h^\beta}.$$

For $(m = 0, \ldots, N)$, the above equation provides a rectangular system of $\left\{C_{-1}^{n+1}, C_0^{n+1}, \ C_1^{n+1}, \ldots, C_{N+1}^{n+1}\right\}$. The BCs are used to obtained two more constraints for finding a unique solution of the system, which are given below:

$$G(x_0, t_{n+1}) = R_1 C_{-1}^{n+1} + R_2 C_0^{n+1} + R_1 C_1^{n+1} = \phi_1(t_{n+1}), \tag{4.4}$$

$$G(x_N, t_{n+1}) = R_1 C_{N-1}^{n+1} + R_2 C_N^{n+1} + R_1 C_{N+1}^{n+1} = \phi_2(t_{n+1}). \tag{4.5}$$

The initial vector can be obtained by the procedure as described in pervious section.

4.2. Stability analysis

From the methodology of previous section, we can proceed by substituting

$$C_m^n = \xi_n e^{im\phi h}. \tag{4.6}$$

in homogenous case of (4.3), which will have the form

$$\begin{aligned}
&(R_1\xi_{n+1}e^{-i\phi h} + R_1\xi_{n+1}e^{i\phi h} + R_2\xi_{n+1}) - (R_1\xi_n e^{-i\phi h} + R_1\xi_n e^{i\phi h} + R_2\xi_n)\\
&+\eta_1\left(\sum_{p=0}^{m+1} w_p^{\alpha} e^{(-p+1)i\phi h}(R_1\xi_{n+1}e^{-i\phi h} + R_2\xi_{n+1} + R_1\xi_{n+1}e^{i\phi h})\right.\\
&\left.+\sum_{p=0}^{N-m+1} w_p^{\alpha} e^{(p-1)i\phi h}(R_1\xi_{n+1}e^{-i\phi h} + R_2\xi_{n+1} + R_1\xi_{n+1}e^{i\phi h})\right)\\
&+\eta_2\left(\sum_{p=0}^{m} w_p^{\beta} e^{(-p)i\phi h}(R_1\xi_{n+1}e^{-i\phi h} + R_2\xi_{n+1} + R_1\xi_{n+1}e^{i\phi h})\right.\\
&\left.+\sum_{p=0}^{N-m} w_p^{\beta} e^{(p)i\phi h}(R_1\xi_{n+1}e^{-i\phi h} + R_2\xi_{n+1} + R_1\xi_{n+1}e^{i\phi h})\right) = 0.
\end{aligned} \tag{4.7}$$

Simplifying the above relation, we get

$$\begin{aligned}
&\xi_{n+1} - \xi_n + \eta_1\left(\sum_{p=0}^{m+1} w_p^{\alpha} e^{(-p+1)i\phi h}\xi_{n+1} + \sum_{p=0}^{N-m+1} w_p^{\alpha} e^{(p-1)i\phi h}\xi_{n+1}\right)\\
&+\eta_2\left(\sum_{p=0}^{m} w_p^{\beta} e^{(-p)i\phi h}\xi_{n+1} + \sum_{p=0}^{N-m} w_p^{\beta} e^{(p)i\phi h}\xi_{n+1}\right) = 0,
\end{aligned}$$

which can also be written as

$$\xi_{n+1} - \xi_n + C_1\xi_{n+1} + C_2\xi_{n+1} + C_3\xi_{n+1} + C_4\xi_{n+1} = 0,$$

where

$$C_1 = \eta_1 \sum_{p=0}^{m+1} w_p^{\alpha} e^{(-p+1)i\phi h}, \qquad C_2 = \eta_1 \sum_{p=0}^{N-m+1} w_p^{\alpha} e^{(p-1)i\phi h},$$

$$C_3 = \eta_2 \sum_{p=0}^{m} w_p^{\beta} e^{(-p)i\phi h}, \qquad C_4 = \eta_2 \sum_{p=0}^{N-m} w_p^{\beta} e^{(p)i\phi h}.$$

Hence

$$\xi_{n+1} = \frac{\xi_n}{(1 + C_1 + C_2 + C_3 + C_4)}. \tag{4.8}$$

So, we get $\xi_{n+1} < |\xi_n|$ because $\mu = (1 + C_1 + C_2 + C_3 + C_4) > 1$.

This concludes that the system is unconditionally convergent.

4.3. Convergence of the scheme

The convergence estimates for the proposed scheme is presented here for the homogenous case:

Theorem 4.1. *Let $\{G(x, t^n)\}_{n=0}^{M}$ be the exact solution of the problem and let $\{G^n\}$ be the approximate solution of proposed problem, then*

$$\|e^{n+1}\| \leqslant \frac{1}{D}\|e^n\|$$

where $e^{n+1} = \{|G(x_m, t^{n+1}) - G_m^{n+1}|; \ \ m = 0, 1, \ldots, N\}$ and

$$D = \left(1 + \eta_1 \left(\sum_{p=0}^{m+1} w_p^{\alpha} + \sum_{p=0}^{N-m+1} w_p^{\alpha}\right) + \eta_2 \left(\sum_{p=0}^{m} w_p^{\beta} + \sum_{p=0}^{N-m} w_p^{\beta}\right)\right).$$

Proof. For the proposed problem, let the exact solution satisfies the numerical scheme (4.2), then we have

$$\begin{aligned} \frac{G(x_m, t_{n+1}) - G(x_m, t_n)}{\tau} &= -\frac{K_\alpha}{2\cos(\frac{\pi\alpha}{2})h^\alpha}\left(\sum_{p=0}^{m+1} w_p^{\alpha} G(x_{m-p+1}, t^{n+1}) + \sum_{p=0}^{N-m+1} w_p^{\alpha} G(x_{m+p-1}, t^{n+1})\right) \\ &\quad -\frac{K_\beta}{2\cos(\frac{\pi\beta}{2})h^\beta}\left(\sum_{p=0}^{m} w_p^{\beta} G(x_{m-p}, t^{n+1}) + \sum_{p=0}^{N-m} w_p^{\beta} G(x_{m+p}, t^{n+1})\right) \end{aligned}$$

or

$$\begin{aligned} G(x_m, t_{n+1}) - G(x_m, t_n) &= -\eta_1\left(\sum_{p=0}^{m+1} w_p^{\alpha} G(x_{m-p+1}, t^{n+1}) + \sum_{p=0}^{N-m+1} w_p^{\alpha} G(x_{m+p-1}, t^{n+1})\right) \\ &\quad -\eta_2\left(\sum_{p=0}^{m} w_p^{\beta} G(x_{m-p}, t^{n+1}) + \sum_{p=0}^{N-m} w_p^{\beta} G(x_{m+p}, t^{n+1})\right) \end{aligned}$$

and

$$G_m^{n+1} - G_m^n = -\eta_1\left(\sum_{p=0}^{m+1} w_p^{\alpha} G_{m-p+1}^{n+1} + \sum_{p=0}^{N-m+1} w_p^{\alpha} G_{m+p-1}^{n+1}\right) - \eta_2\left(\sum_{p=0}^{m} w_p^{\beta} G_{m-p}^{n+1} + \sum_{p=0}^{N-m} w_p^{\beta} G_{m+p}^{n+1}\right).$$

Subtracting above two equations gives

$$e^{n+1} = e^n - \eta_1\left(\sum_{p=0}^{m+1} w_p^{\alpha} e^{n+1} + \sum_{p=0}^{N-m+1} w_p^{\alpha} e^{n+1}\right) - \eta_2\left(\sum_{p=0}^{m} w_p^{\beta} e^{n+1} + \sum_{p=0}^{N-m} w_p^{\beta} e^{n+1}\right),$$

where $e^{n+1} = \max\{|G(x_m, t^{n+1}) - G_m^{n+1}|; \ \ m = 0, 1, \ldots, N\}$. Taking the inner product with e^{n+1} on both sides and using the fact that $\langle y, y\rangle = \|y\|^2$, we have

$$\begin{aligned}
\langle e^{n+1}, e^{n+1}\rangle &= \langle e^{n}, e^{n+1}\rangle - \eta_1\left(\sum_{p=0}^{m+1} w_p^{\alpha}\langle e^{n+1}, e^{n+1}\rangle + \sum_{p=0}^{N-m+1} w_p^{\alpha}\langle e^{n+1}, e^{n+1}\rangle\right)\\
&\quad -\eta_2\left(\sum_{p=0}^{m+} w_p^{\beta}\langle e^{n+1}, e^{n+1}\rangle + \sum_{p=0}^{N-m} w_p^{\beta}\langle e^{n+1}, e^{n+1}\rangle\right)\\
\|e^{n+1}\|^2 &= \langle e^{n}, e^{n+1}\rangle - \eta_1\left(\sum_{p=0}^{m+1} w_p^{\alpha}\|e^{n+1}\|^2 + \sum_{p=0}^{N-m+1} w_p^{\alpha}\|e^{n+1}\|^2\right)\\
&\quad -\eta_2\left(\sum_{p=0}^{m} w_p^{\beta}\|e^{n+1}\|^2 + \sum_{p=0}^{N-m} w_p^{\beta}\|e^{n+1}\|^2\right),\\
\|e^{n+1}\|^2 &\leqslant \|e^{n}\|\|e^{n+1}\| - \eta_1\left(\sum_{p=0}^{m+1} w_p^{\alpha}\|e^{n+1}\|^2 + \sum_{p=0}^{N-m+1} w_p^{\alpha}\|e^{n+1}\|^2\right)\\
&\quad -\eta_2\left(\sum_{p=0}^{m} w_p^{\beta}\|e^{n+1}\|^2 + \sum_{p=0}^{N-m} w_p^{\beta}\|e^{n+1}\|^2\right).
\end{aligned}$$

Dividing by $\|e^{n+1}\|$ gives

$$\|e^{n+1}\| \leqslant \|e^{n}\| - \|e^{n+1}\|\left(\eta_1\left(\sum_{p=0}^{m+1} w_p^{\alpha} + \sum_{p=0}^{N-m+1} w_p^{\alpha}\right) + \eta_2\left(\sum_{p=0}^{m} w_p^{\beta} + \sum_{p=0}^{N-m} w_p^{\beta}\right)\right),$$

which means

$$\begin{aligned}
\|e^{n+1}\|\left(1 + \eta_1\left(\sum_{p=0}^{m+1} w_p^{\alpha} + \sum_{p=0}^{N-m+1} w_p^{\alpha}\right) + \eta_2\left(\sum_{p=0}^{m} w_p^{\beta} + \sum_{p=0}^{N-m} w_p^{\beta}\right)\right) &\leqslant \|e^{n}\|,\\
\|e^{n+1}\| &\leqslant \frac{1}{D}\|e^{n}\|.
\end{aligned}$$

It is clear that $D \geqslant 1$, hence the proposed scheme is convergent. □

4.4. Example 2

Consider the following example [12]

$$\frac{\partial G(x,t)}{\partial t} = K_{\alpha}\frac{\partial^{\alpha} G(x,t)}{\partial |x|^{\alpha}} + K_{\beta}\frac{\partial^{\beta} G(x,t)}{\partial |x|^{\beta}} + f(x,t) \tag{4.9}$$

with BCs and IC

$$G(0,t) = G(1,t) = G(x,0) = 0 \tag{4.10}$$

where

$$
\begin{aligned}
f(x,t) \quad &= \frac{K_\alpha t^\alpha e^{\beta t}}{2\cos(\frac{\alpha\pi}{2})}\left(\frac{2}{(2-\alpha)!}(x^{2-\alpha}+(1-x)^{2-\alpha})-\frac{12}{(3-\alpha)!}(x^{3-\alpha}+(1-x)^{3-\alpha})\right.\\
&\left.+\frac{24}{(4-\alpha)!}(x^{4-\alpha}+(1-x)^{4-\alpha})\right)+\frac{K_\beta t^\alpha e^{\beta t}}{2\cos(\frac{\beta\pi}{2})}\left(\frac{2}{(2-\beta)!}(x^{2-\beta}+(1-x)^{2-\beta})\right.\\
&\left.-\frac{12}{(3-\beta)!}(x^{3-\beta}+(1-x)^{3-\beta})+\frac{24}{(4-\beta)!}(x^{4-\beta}+(1-x)^{4-\beta})\right)\\
&+t^{\alpha-1}e^{\beta t}(\alpha+\beta t)x^2(1-x)^2. \qquad (4.11)
\end{aligned}
$$

The exact solution is $G(x,t) = t^\alpha e^{\beta t}x^2(1-x)^2$. Table 7 shows the absolute errors at different values of γ, which indicates that the results are nearly same for different values of γ. Table 8 for $N = 40$ shows the numerical display of absolute errors of the RSF-ADE for different values of α in example 2. Similarly Table 9 describes the numerical display of absolute errors for $N = 40$ and $T = 0.001$ at different values of α. From these tables, we see that the solution is better for smaller values of T. Table 10 is providing the comparison between the maximum error of the approximate solution and solution in [12].

Figure 2(a) shows the geometrical representation of error for $N = 2^6$, $T = 0.001$ at different values of α, which indicates that by increasing the value of α the approximate solution move closer to exact one. Geometrical representation of both solutions for $N = 2^6$ is shown in Figure 2(b) which indicates that exact and approximate solution are very much coinciding.

Table 7. The absolute errors for $N = 40$ of example 2 at $\alpha = 1.2$.

x	$\gamma = 0$	$\gamma = 0.5$	$\gamma = 1.0$
0.00	3.159600×10^{-6}	3.162500×10^{-6}	3.162000×10^{-6}
0.20	5.093256×10^{-7}	5.137735×10^{-7}	5.130321×10^{-7}
0.40	7.738800×10^{-6}	7.730800×10^{-6}	7.732100×10^{-6}
0.60	1.583960×10^{-5}	1.582100×10^{-5}	1.582410×10^{-5}
0.80	1.741160×10^{-5}	1.73353×10^{-5}	1.734800×10^{-5}
1.00	2.208280×10^{-7}	2.780499×10^{-4}	2.316613×10^{-4}

Table 8. The absolute errors for $T = 0.01$ and $N = M = 40$ of example 2 at different values of α.

x	$\alpha = 1.2$	$\alpha = 1.4$	$\alpha = 1.6$	$\alpha = 1.8$
0.00	3.159600×10^{-6}	1.490700×10^{-6}	7.661871×10^{-7}	4.208717×10^{-7}
0.20	5.093256×10^{-7}	8.594544×10^{-8}	6.913968×10^{-8}	6.039970×10^{-8}
0.40	7.738800×10^{-6}	4.241300×10^{-6}	2.000800×10^{-6}	8.989871×10^{-7}
0.60	1.583960×10^{-5}	8.549800×10^{-6}	4.103000×10^{-6}	1.894400×10^{-6}
0.80	1.741160×10^{-5}	9.436500×10^{-6}	4.688200×10^{-6}	2.283700×10^{-6}
1.00	2.208280×10^{-7}	7.396369×10^{-7}	6.778882×10^{-7}	1.776700×10^{-6}

Table 9. The absolute errors for $N = M = 40$ and $T = 0.001$ of example 2 at different values of α.

x	$\alpha = 1.2$	$\alpha = 1.4$	$\alpha = 1.6$	$\alpha = 1.8$
0.00	1.921803×10^{-8}	5.660408×10^{-9}	1.848237×10^{-9}	6.547472×10^{-10}
0.20	8.371194×10^{-8}	3.361751×10^{-8}	1.040720×10^{-8}	2.976077×10^{-9}
0.40	3.525233×10^{-7}	1.355650×10^{-7}	4.199897×10^{-8}	1.215795×10^{-8}
0.60	6.204239×10^{-7}	2.374454×10^{-7}	7.367459×10^{-8}	2.139819×10^{-8}
0.80	6.301783×10^{-7}	2.409092×10^{-7}	7.511775×10^{-8}	2.199683×10^{-8}
1.00	8.868589×10^{-8}	3.273835×10^{-8}	1.040274×10^{-8}	3.472292×10^{-9}

Table 10. Comparison of the maximum error of example 2 of proposed scheme with the solution from [12].

$h = 1/N$	$L1/L2$ [12]	Standard/Shifted Grunwald [12]	Proposed scheme
$\frac{1}{50}$	1.8144(−2)	2.8191(−3)	4.1574(−3)
$\frac{1}{100}$	9.4917(−3)	1.5093(−3)	9.3134(−4)
$\frac{1}{200}$	4.8584(−3)	7.7821(−4)	4.1598(−4)
$\frac{1}{400}$	2.4586(−3)	3.9459(−4)	1.0234(−4)

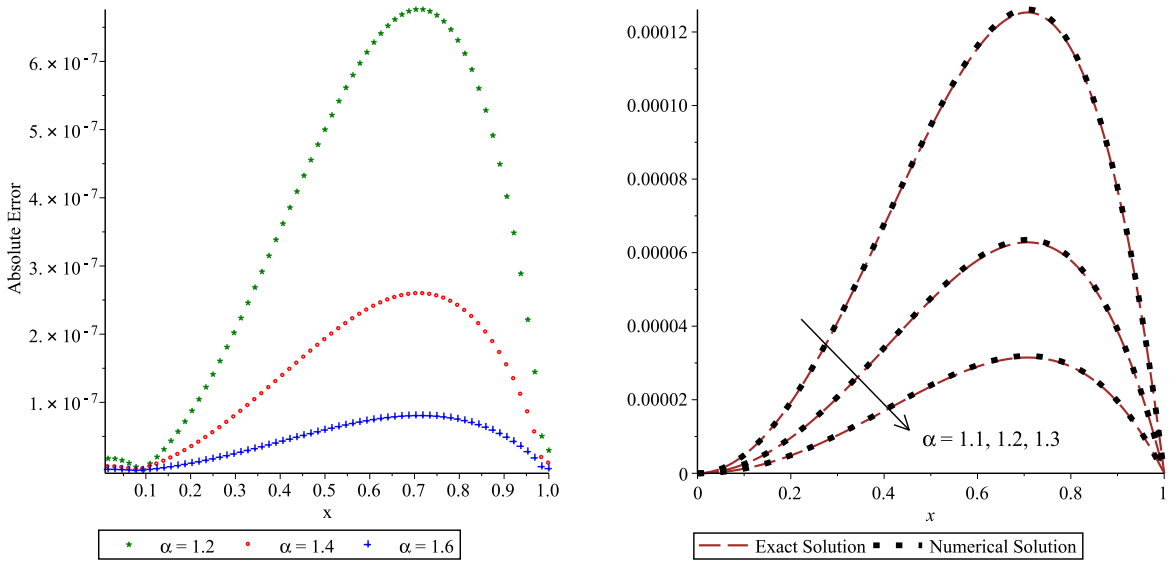

(a) Errors (b) Comparison of solutions

Figure 2. Geometrical representation of example 2. (a) For $N = 2^6$ and $T = 0.001$ at different values of α. (b) Comparison of both solutions at $N = 2^6$ and $T = 0.001$.

Algorithm: Hybrid B-spline collocation method for RSF-DE and RSF-ADE

(1) Discretize x_i, t_j for $i = 0, 1, \ldots, N$, $j = 0, 1, \ldots, M$.
(2) Evaluate w_p^{α}, $p = 0, 1, \ldots, N$ for RSF-DE ($w_p^{\alpha}, w_p^{\beta}$, $p = 0, 1, \ldots, N$ for RSF-ADE).
(3) Initialize the vector $C^0 = [C_{-1}^0, C_0^0, \ldots, C_{N+1}^0]$ using initial conditions and Thomas algorithm.
(4) Discretize $G(x_m, t_{n+1})$ and replace by $R_1 C_{m-1}^{n+1} + R_2 C_m^{n+1} + R_1 C_{m+1}^{n+1}$ for $k = 0, 1, \ldots, M-1$.
(5) For $i = 1, 2, \ldots, N-1$
   (a) Construction of square system of equations using (3.2) for RSF-DE and (4.2) for RSF-ADE,
   (b) Using fsolve evaluate the solution at each time level till final time.
(6) Substitute in B-spline basis function (2.1).

5. Conclusions and future work

The aim of this research was to solve RSF-DE and RSF-ADE using HBCM. We have used the left and right sided Riemann Liouville formulae to discretize the Riesz fractional derivative. The discretized equation is then updated with the spanning form of hybrid B-spline basis. The convergence of numerical scheme is ensured by using VN stability analysis. The methods are employed on numerical examples of both models to show the applicability of prescribed method. The results are displayed using different tables, which shows that solution becomes convergent by decreasing the values of T. Numerical results are also shown graphically, which indicate that the approximate solutions are very much coinciding with the exact solution. The comparison provided in Tables 6 and 10 with [12] indicate that approximate solution are comparable. The display of CPU time and Memory allocation is placed in Table 11. However, the proposed numerical algorithms can be extended for tempered fractional diffusion equation [32] with some adjustments.

Table 11. Display of CPU time(s) and Memory(kb) of proposed scheme for the solution of RSF-DE and RSF-ADE for $T = 0.1$.

N	M	RSF-DE		RSF-ADE	
		CPU	Memory	CPU	Memory
2^4	2^5	2.39	649	4.19	904
	2^6	9.48	1845	8.27	2012
2^5	2^5	6.79	1241	9.63	1024
	2^6	13.45	2575	17.84	2521
2^6	2^5	9.79	1920	16.73	2840
	2^6	23.71	2908	28.41	4215

Acknowledgments

This work is supported by the Higher Education Commission of Pakistan under the NRPU project grant number 9306/Punjab/NRPU/R&D/HEC/2017.

Conflict of interest

The authors declare no conflicts of interest.

References

1. Y. Lin, C. Xu, Finite difference/spectral approximations for the time-fractional diffusion equation, *J. Comput. Phys.*, **225** (2007), 1533–1552. https://doi.org/10.1016/j.jcp.2007.02.001
2. N. J. Ford, J. A. Connolly, Systems-based decomposition schemes for the approximate solution of multi-term fractional differential equations, *J. Comput. Appl. Math.*, **229** (2009), 382–391. https://doi.org/10.1016/j.cam.2008.04.003
3. S. Esmaeili, M. Shamsi, A pseudo-spectral scheme for the approximate solution of a family of fractional diffusion equations, *Commun. Nonlinear Sci. Numer. Simul.*, **16** (2011), 3646–3654. https://doi.org/10.1016/j.cnsns.2010.12.008
4. R. Hilfer, *Applications of fractional calculus in physics*, World Scientific Press, 2000.
5. R. Magin, Y. Sagher, S. Boregowda, *Application of fractional calculus in modeling and solving the bioheat equation*, WIT Press, 2004.
6. F. Liu, V. Anh, I. Turner, Numerical solution of the space fractional Fokker-Planck equation, *J. Comput. Appl. Math.*, **166** (2004), 209–219. https://doi.org/10.1016/j.cam.2003.09.028
7. A. Akgul, S. A. Khoshnaw, Application of fractional derivative on non-linear biochemical reaction models, *Int. J. Intell. Networks*, **1** (2020), 52–58. https://doi.org/10.1016/j.ijin.2020.05.001
8. E. Barkai, R. Metzler, J. Klafter, From continuous time random walks to the fractional Fokker-Planck equation, *Phys. Rev. E*, **61** (2000), 132–138. https://doi.org/10.1103/PhysRevE.61.132
9. R. Metzler, J. Klafter, Boundary value problems for fractional diffusion equations, *Phys. A: Stat. Mech. Appl.*, **278** (2000), 107–125. https://doi.org/10.1016/S0378-4371(99)00503-8
10. G. M. Zaslavsky, Chaos, fractional kinetics, and anomalous transport, *Phys. Rep.*, **371** (2002), 461–580. https://doi.org/10.1016/S0370-1573(02)00331-9
11. A. I. Saichev, G. M. Zaslavsky, Fractional kinetic equation: Solutions and applications, *Chaos*, **7** (1997), 753–764. https://doi.org/10.1063/1.166272
12. Q. Yang, F. Liu, I. Turner, Numerical methods for fractional partial differential equations with Riesz space fractional derivatives, *Appl. Math. Model.*, **34** (2010), 200–218. https://doi.org/10.1016/j.apm.2009.04.006
13. S. Shen, F. Liu, V. Anh, I. Turner, The fundamental solution and numerical solution of the Riesz fractional advection dispersion equation, *IMA J. Appl. Math.*, **73** (2008), 850–872. https://doi.org/10.1093/imamat/hxn033
14. H. Zhang, F. Liu, V. Anh, Galerkin finite element approximation of symmetric space-fractional partial differential equations, *Appl. Math. Comput.*, **217** (2010), 2534–2545. https://doi.org/10.1016/j.amc.2010.07.066

15. H. F. Ding, Y. X. Zhang, New numerical methods for the Riesz space fractional partial differential equations, *Comput. Math. Appl.*, **63** (2012), 1135–1146. https://doi.org/10.1016/j.camwa.2011.12.028

16. H. L. Liao, P. Lyn, S. Vong, Second-order BDF time approximation for Riesz space-fractional diffusion equations, *Int. J. Comput. Math.*, **95** (2018), 144–158. https://doi.org/10.1080/00207160.2017.1366461

17. X. M. Gu, Y. L. Zhao, X. L. Zhao, B. Carpetieri, Y. Y. Huang, A note on parallel preconditioning for the all-at-once solution of Riesz fractional diffusion equations, *Numer. Math. Theor. Meth. Appl.*, **14** (2021), 893–919. https://doi.org/10.4208/nmtma.OA-2020-0020

18. Y. Y. Huang, X. M. Gu, U. Gong, H. Li, Y. L. Zhao, B. Carpentieri, A fast preconditioned semi-implicit difference scheme for strongly nonlinear space-fractional diffusion equations, *Fractal Fract.*, **5** (2021), 230. https://doi.org/10.3390/fractalfract5040230

19. H. Y. Jian, T. Z. Huang, X. M. Gu, Y. L. Zhao, Fast compact implicit integration factor method with non-uniform meshes for the two-dimensional nonlinear Riesz space-fractional reaction diffusion equation, *Appl. Numer. Math.*, **156** (2020), 346–363. https://doi.org/10.1016/j.apnum.2020.05.005

20. H. Y. Jian, T. Z. Huang, X. M. Gu, X. L. Zhao, Y. L. Zhao, Fast implicit integration factor method for nonlinear space Riesz fractional reaction-diffusion equations, *J. Comput. Appl. Math.*, **378** (2020), 112935. https://doi.org/10.1016/j.cam.2020.112935

21. H. Y. Jian, T. Z. Huang, A. Ostermann, X. M. Gu, Y. L. Zhao, Fast IIF-WENO method on non-uniform meshes for nonlinear space-fractional convection diffusion reaction equations, *J. Sci. Comput.*, **89** (2021), 13. https://doi.org/10.1007/s10915-021-01622-9

22. W. K. Zahra, S. M. Elkholy, The use of cubic splines in the numerical solution of fractional differential equations, *Int. J. Maths. Math. Sci.*, **2012** (2012), 638026. https://doi.org/10.1155/2012/638026

23. M. Abbas, A. A. Majid, A. Rashid, Numerical method using cubic trigonometric B-spline technique for nonclassical diffusion problems, *Abst. Appl. Anal.*, **2014** (2014), 849682. https://doi.org/10.1155/2014/849682

24. T. Nazir, M. Abbas, A. I. M. Ismail, A. A. Majid, A. Rashid, The numerical solution of advection-diffusion problems using new cubic trigonometric B-splines approach, *Appl. Math. Model.*, **40** (2016), 4586–4611. https://doi.org//10.1016/j.apm.2015.11.041

25. X. Zhu, Y. Nie, Z. Yuan, J. Wang, Z. Yang, An exponential B-spline collocation method for the fractional sub-diffusion equation, *Adv. Differ. Equ.*, **2017** (2017), 285. https://doi.org/10.1186/s13662-017-1328-6

26. M. Yaseen, M. Abbas, T. Nazir, D. Baleanu, A finite difference scheme based on cubic trigonometric B-splines for a time fractional diffusion-wave equation, *Adv. Differ. Equ.*, **2017** (2017), 274. https://doi.org/10.1186/s13662-017-1330-z

27. M. S. Hashmi, M. Awais, A. Waheed, Q. Ali, Numerical treatment of Hunter Saxton equation using cubic trigonometric B-spline collocation method, *AIP Adv.*, **7** (2017), 095124. https://doi.org/10.1063/1.4996740

28. R. Shikrani, M. S. Hashmi, N. Khan, A. Ghaffar, K. S. Nisar, J. Singh, et al., An efficient numerical approach for space fractional partial differential equations, *Alex. Eng. J.*, **59** (2020), 2911–2919. https://doi.org/10.1016/j.aej.2020.02.036

29. M. S. Hashmi, Z. Shehzad, A. Ashraf, Z. Zhang, Y. P. Lv, A. Ghaffar, et al., A new variant of B-spline for the solution of modified fractional Anomalous subdiffusion equation, *J. Funct. Spaces*, **2021** (2021), 8047727. https://doi.org/10.1155/2021/8047727

30. M. S. Hashmi, M. Wajiha, S. W. Yao, A. Ghaffar, M. Inc, Cubic spline based differential quadrature method: A numerical approach for fractional Burger equation, *Results Phys.*, **26** (2021), 104415. https://doi.org/10.1016/j.rinp.2021.104415

31. M. S. Hashmi, U. Aslam, J. Singh, K. S. Nisar, An efficient numerical scheme for fractional model of telegraph equation, *Alex. Eng. J.*, **61** (2022), 6383–6393. https://doi.org/10.1016/j.aej.2021.11.065

32. Y. L. Zhao, P. Y. Zhu, X. M. Gu, X. L. Zhao, H. Y. Jian, A preconditioning technique for all-at-once system from the nonlinear tempered fractional diffusion equation, *J. Sci. Comput.*, **83** (2020), 10. https://doi.org/10.1007/s10915-020-01193-1

AIMS Press